Determination of geometrical and kinematical properties of halo coronal mass ejections using the cone model

X. P. Zhao
W. W. Hansen Experimental Physics Laboratory, Stanford University, Stanford, California, USA

S. P. Plunkett
Universities Space Research Association, Naval Research Laboratory, Washington, D.C., USA

W. Liu
W. W. Hansen Experimental Physics Laboratory, Stanford University, Stanford, California, USA

Received 25 October 2001; revised 8 February 2002; accepted 12 February 2002; published 31 August 2002.

[1] Many broadside coronal mass ejections (CMEs) propagate almost radially beyond the first couple of solar radii, and their angular widths remain nearly constant while propagating through the corona. Assuming that these characteristics hold true for halo CMEs that originate far from solar limbs, some useful geometric and kinematic properties of halo CMEs may be reproduced using a simple geometrical model of a CME as a cone. The cone model uses three free parameters, characterizing the angular width and the central position of the halo CME. These geometric properties can be determined by matching the observed halos at a series of times with the modeled halos for a series of radial distances. The kinematic properties, the radial velocity and acceleration, of the halo CME can also be determined on the basis of the series of times and radial distances. These properties are important for predicting the geoeffectiveness of a halo CME and cannot be observed directly with currently available instrumentation. As a test, the geometric and kinematic properties of the 12 May 1997 halo CME have been inferred using the cone model. This shows that the cone model does provide a new way of testing our understanding of halo CMEs, though there are limitations for some halo CMEs. *INDEX TERMS:* 7513 Solar Physics, Astrophysics, and Astronomy: Coronal mass ejections; 7524 Solar Physics, Astrophysics, and Astronomy: Magnetic fields; 7519 Solar Physics, Astrophysics, and Astronomy: Flares; 7531 Solar Physics, Astrophysics, and Astronomy: Prominence eruptions; *KEYWORDS:* halo coronal mass ejection, angular width, central position, radial speed, the cone model

1. Introduction

[2] The first halo coronal mass ejection (CME) was detected with the SOLWIND coronagraph on 27 November 1979. This halo CME was a bright cloud surrounding the entire Sun and propagating outward from it in all directions, and was interpreted as a broad shell or bubble of dense plasma ejected directly toward (or away from) the Earth [*Howard et al.*, 1982]. A broad interplanetary disturbance produced by this halo CME was detected with the Helios photometers and the disturbance traveled along the Sun-Earth line toward the Earth, where it generated a small geomagnetic storm [*Jackson*, 1985]. These observations suggest that the interpretation of the halo CME as lying out of the plane of the sky and being Earth-directed is acceptable.

[3] Halo CMEs, many of which are very faint, can now be routinely observed with the Large Angle Spectrometric Coronagraph (LASCO), due to its high sensitivity and wide dynamic range [*Brueckner et al.*, 1995]. The source regions of the halo CMEs are believed to be associated with surface activities, such as flares and solar filament disappearances, and can thus be studied using observations of the solar disk by Yohkoh/SXT and SOHO/the Extreme Ultraviolet Imaging Telescope (EIT) [*Delaboudiniere et al.*, 1995] as well as in the H_α line at various solar observatories on the ground [e.g., *Hudson et al.*, 1998; *Cane et al.*, 1998; *Webb et al.*, 2001]. The combination of LASCO and EIT observations of halo CMEs makes it possible to determine whether or not a halo CME originated on the front side of the solar disk [*Plunkett et al.*, 2001]. The close relationship of front-side halo CMEs, magnetic clouds, and magnetic storms has been demonstrated recently [*Webb et al.*, 2000; *Zhao and Webb*, 2000], further suggesting that the central position of halo CMEs is located far away from the solar limb.

[4] The increased solar wind speed associated with front-side halo CMEs is one of the key parameters that determine the geoeffectiveness of the CMEs. By using the technique similar to the one developed by *Gopalswamy et al.* [2000] such increased solar wind speed may be inferred more accurately if the geometrical and kinematical properties of the halo CMEs can be determined.

0148-0227/02/2001JA009143$09.00

[5] For broadside CMEs, i.e., the CMEs with the latitudinal span of their bright feature in the plane of the sky being less than 120°, their geometric properties, the angular width and the central position angle, can be directly measured based on their latitudinal span: the latitudinal span is the measure of the angular width of the broadside CMEs, and the bisector of the span is defined to be the central position angle (measured counterclockwise from the projection of the Sun's north pole) of the broadside CMEs. It should be noted that unless the real central position or source location of a broadside CME is located exactly at solar limbs, both the angular width and the central position angle measured in this way are apparent ones. The real angular width and central position for both partial and full halo CMEs, i.e., the CMEs with the latitudinal span greater than 120°, can not be measured directly from white-light images. The central position of halo CMEs is often assumed to be located near the center of the solar disk or near the associated surface activities such as solar flares, though it has been reported that CME-associated flares or active regions are often located near one leg of CMEs, rather than near the center [*Harrison*, 1986; *Plunkett et al.*, 2001].

[6] The speed profiles of CMEs are often derived by choosing a specific feature in a time-lapse movie and tracking its position outward with time. A new technique for deriving speed profiles from LASCO observations has been developed recently. By choosing a radial slice with a specific position angle from each difference LASCO image and merging all those slices, the resulting synoptic grey-scale maps show the tracks of all of detectable features that move along the chosen radial path, free from observational selection and bias [*Sheeley et al.*, 1999, and references therein]. For broadside CMEs the measured velocity and acceleration are nearly radial directed; they are, however, projected against the plane of the sky for halo CMEs.

[7] The cone model developed in the next section may provide a way to determine the real angular width, central position angle, and the radial speed and acceleration for halo CMEs.

2. Cone Model

[8] Many broadside CMEs observed by LASCO propagate almost radially through the C2 and C3 fields of view (C2: 2.0–6.0 $R_\odot$ and C3: 3.7–30.0 $R_\odot$). However, there are some broadside CMEs that begin at midlatitude near the edge of the streamer belt near solar minimum and have shown clear nonradial motion in the first couple of solar radii [*Plunkett et al.*, 1997]. A tally of the number of CMEs showing nonradial motions in the inner corona is 118 among 841 CMEs observed between 1996 and 1998. Since only events with significant (i.e., at least 10°) nonradial motions were noted, the ratio of 14% is likely a lower limit [*St. Cyr et al.*, 2000]. The angular width of many broadside CMEs remains constant while the CMEs propagate outward [*Webb et al.*, 1997]. The angular width of interplanetary plasma clouds is comparable to that of CMEs near the Sun [*Webb and Jackson*, 1990], suggesting that the angular width of CMEs remains constant as they propagate outward from the Sun, especially in the outer corona. Many full halo CMEs have a nearly round halo, suggesting that the latitudinal angular width is basically the same as the ecliptic angular width, i.e., the shell or bubble of dense plasma is nearly symmetric about the central position of CMEs. It is thus reasonable to assume that (1) the central position of halo CMEs observed by LASCO, especially in the outer corona or in C3 field of view, is located somewhere near both the CME-associated active region and the center of the solar disk, (2) their bulk velocities point radially, and (3) their angular widths remain constant while the CMEs propagate through the corona. The boundary of emission observed by LASCO for halo CMEs should form a cone of constant angular spread, and the apex (the point the cone narrows to from a round cross section) of the cone is located at the center of the Sun. The concept of the cone model has been used in estimating the mass and other physical properties of CMEs [*Howard et al.*, 1982; *Fisher and Munro*, 1984].

[9] In the heliographic coordinate system ($X_hY_hZ_h$) with its origin located at the Sun's center and Z_h and X_h axes pointed to the north and the Earth, respectively, the Y_hZ_h plane denotes the plane of the sky. The orientation of the central axis of the cone, i.e., the direction from Sun's center to the central position of a CME near the solar surface, can be described using two parameters in the system: the longitude ϕ measured from the central meridian and the latitude λ. In the cone's coordinate system, $X_cY_cZ_c$, with its origin located at the apex of the cone, the X_c axis aligned with the central axis of the cone and Y_c axis lay in the plane of X_hY_h, the round cross section of the cone at a specific radial distance, r, may be specified using the half of the angular width of the cone, ω,

$$X_c = r\cos(\omega), \tag{1}$$

$$Y_c = r\sin(\omega)\cos(\delta), \tag{2}$$

$$Z_c = r\sin(\omega)\sin(\delta), \tag{3}$$

where δ denotes the azimuthal angle ranging from 0° to 360°. With the angular width and radial distance given, a set of X_c, Y_c and Z_c are uniquely determined, and vice versa. In other words, although there are more than one pair of r and ω that can produce an single pair of Y_c and Z_c, there is only one set of X_c, Y_c and Z_c that corresponds to a pair of r and ω.

[10] The projection of the round cross section onto the plane of the sky can be obtained on the basis of the transformation matrix from system $X_cY_cZ_c$ to system $X_hY_hZ_h$

$$Y_h = X_c\cos\lambda\sin\phi + Y_c\cos\phi - Z_c\sin\lambda\sin\phi, \tag{4}$$

$$Z_h = X_c\sin\lambda + Z_c\cos\lambda. \tag{5}$$

Both Y_h and Z_h depend on X_c as well as Y_c and Z_c. Unless the orientation of the cone (λ, ϕ) is exactly aligned with the line-of-sight, i.e., $\lambda = 0°$ and $\phi = 0°$, the three free parameters in the model, ω, λ and ϕ, can be uniquely determined by matching the observed halo at a specific time with the modeled halo at a corresponding distance, even though more than one pair of r and ω can produce an single pair of Y_c and Z_c. When the orientation of the cone

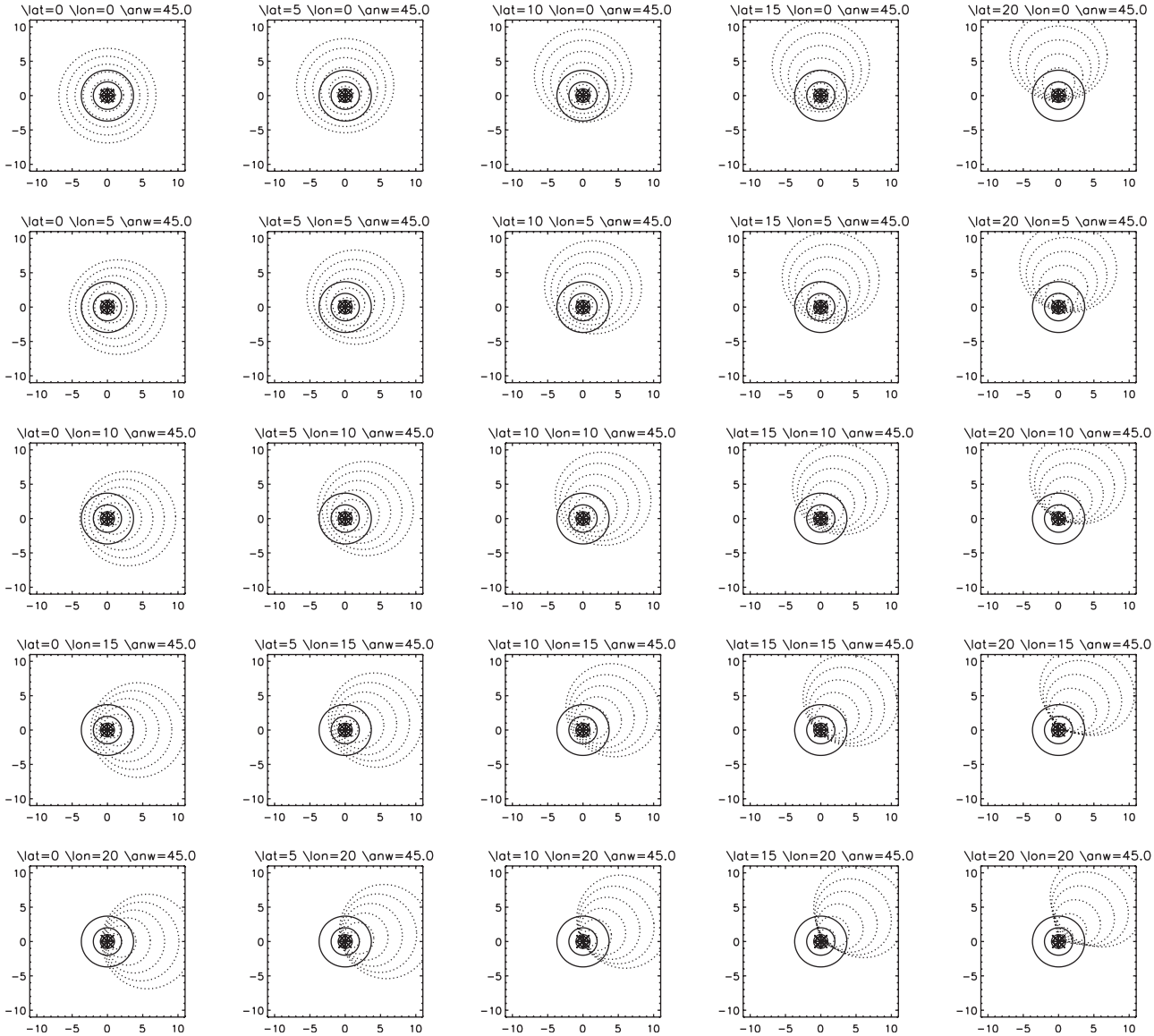

Figure 1. The dependence of the predicted halo (dotted circles or ellipses) on the orientation of the central axis of the cone (the location of the source) expressed by the latitude ('lat') and longitude ('lon'). The angular width ('anw') for all panels is 45°. The latitude (longitude) increases from 0° on the left (0° at the top) to 20° on the right (20° at the bottom). The three solid circles of 1.0, 2.0, 3.7 solar radii in each panel denote the solar disk, the C2 occulting disk, and the C3 occulting disk. The six dotted lines in each panel denote the six cross sections corresponding to the radial distances of 3.0, 6.0, 9.0, 12.0, 15.0, 18.0 solar radii in the cone coordinate system.

is aligned with the line-of-sight, Equations (4) and (5) become

$$Y_h = Y_c, \tag{6}$$

$$Z_h = Z_c. \tag{7}$$

Both Y_h and Z_h depend, respectively, on Y_c and Z_c alone, the solution becomes degenerate and the determination of the angular width is not unique because there are more than one pair of ω and r that could yield an identical pair of Y_h and Z_h. In other words, a faster, narrower CME may have a same halo as a slower, broader CME has in this case.

3. Dependence of the Occurrence of Halo CMEs on the Orientation and Angular Width

[11] It has been shown that the average angular width of white-light broadside CMEs is about 45 degrees [*Howard et al.*, 1985; *Hundhausen*, 1993; *St. Cyr et al.*, 2000]. There is a wide variation of widths about this average. It is instructive to ask what the range of the cental position angle should be for a CME with angular width of 45° to form a halo?

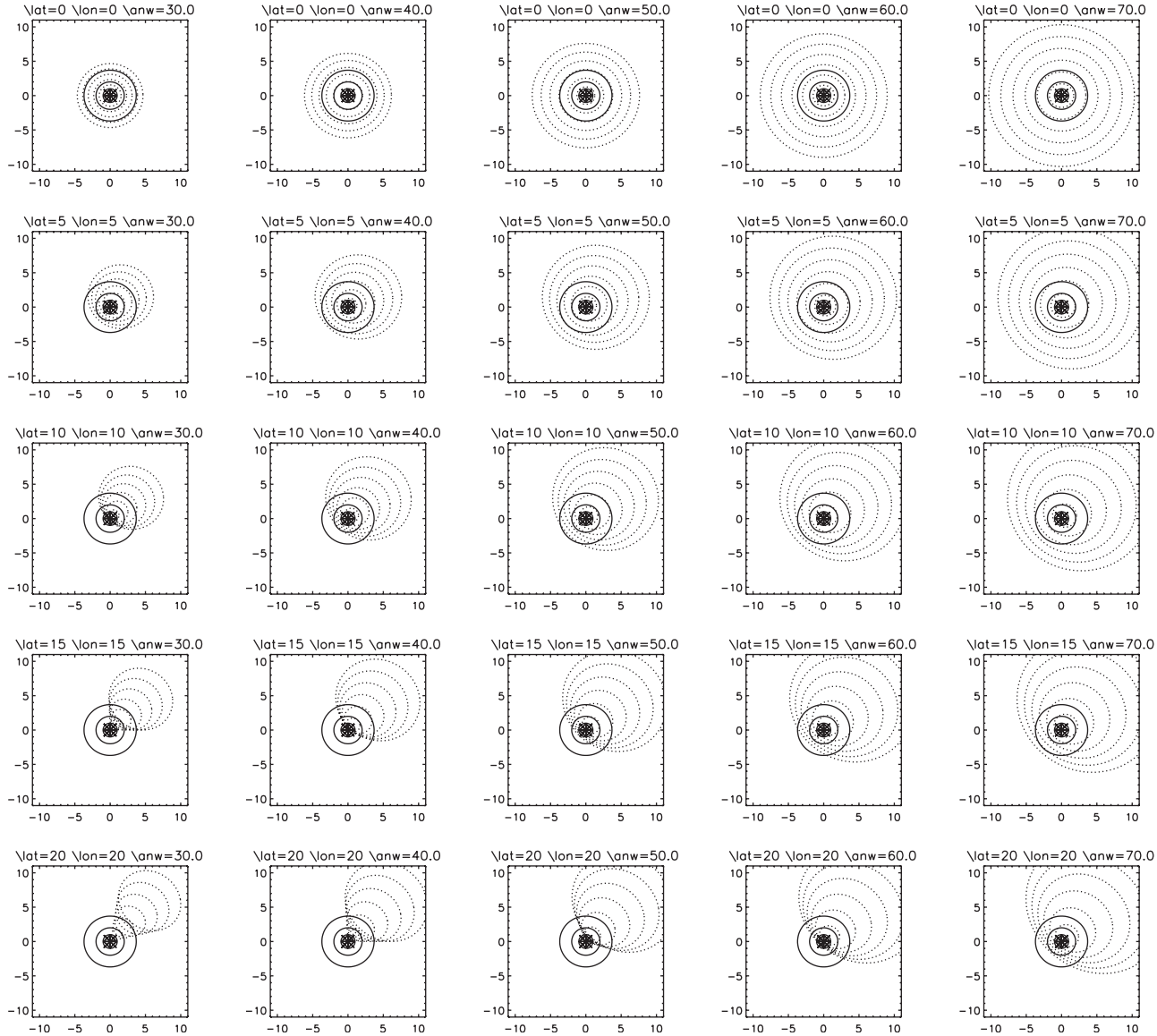

Figure 2. The dependence of the predicted halo (dotted circles or ellipses) on the angular width ('anw'). The symbols lat and lon have same meaning as Figure 1.

[12] Figure 1 shows how the cross section of the cone projected on the plane of the sky changes in shape as the orientation and the radial distance change. The angular width of the cone for all the panels is 45 degrees. The three solid circles in each panel denote, respectively, 1.0, 2.0 and 3.7 solar radii, corresponding to the radius of the solar disk, the C2 occulting disk, and the C3 occulting disk. The six dotted circles or ellipses in each panel denote the six projected cross sections corresponding to the radial distances of 3.0, 6.0, 9.0, 12.0, 15.0, 18.0 solar radii. The dotted circles in the panels from left (top) to right (bottom) show the change in shape caused by the increase of the latitude (longitude). Figure 1 indicates that for a CME with angular width of 45°, full bright rings on the plane of sky may occur only when the source position is within a small circle of radius $\sim$15° away from the disk center (see the nine panels in the top left corner). The halo occurs in C2 (C3) when the CME propagates beyond 3 (6) solar radii. When the angle between the central axis of the cone and the line of sight is between $\sim$15° and $\sim$30° only a partial halo CME can be formed. The right bottom panel shows that the angular width subtended by the dotted arcs is $\simeq$120°, the lowest limit of the angular width that is often adopted as the criterion for a CME to be considered a partial halo CME [*St. Cyr et al.*, 2000]. Thus for halo CMEs that have a true angular width of 45°, the central position is located within a circle of $\sim$15° from the center of solar disk, and for partial halo CMEs, it is located between $\sim$15 and $\sim$30 degrees from the disk center.

[13] Figure 2 shows the effect of the angular width on the shape of the cross section of the cone projected on the plane of the sky. The solid and dotted lines here have the same meaning as in Figure 1. The angular width (the orientation) increases from 30° on the left (0° on the top) to 70° on the

right (20° on the bottom). It indicates that the chance to form full halo CMEs increases as the angular width increases.

4. Geometrical and Kinematical Properties of the 12 May 1997 Halo CME

[14] The 12 May 1997 halo CME [*Plunkett et al.*, 1998] showed a series of expanding bright rings centered near the occulting disk. The CME was first visible in a C2 image recorded at 06:30 UT and in a C3 image recorded at 08:06 UT, respectively. The CME followed an eruptive event observed by EIT in the lower corona at approximately 04:35 UT. The eruptive event was centered on active region 8038 at N23 W07 [*Thompson et al.*, 1998]. Thus this was a front-side halo CME. Figure 3 shows the development of the 12 May 1997 halo CME from 06:45 UT to 15:37 UT, as seen by the LASCO/C3 coronagraph. The images shown in Figures 3 and 4 are differences from a pre-event base image.

[15] To reproduce expanding bright rings between 08:06 UT and 14:51 UT (see Figure 4), the initial test values for the angular width, the latitude, and the longitude are taken to be 45, 5 and 5 degrees, respectively. Then these values are adjusted iteratively to best match the middle of the bright ring observed at all six times. All black circles in Figure 4 are the cross sections of the cone computed at different distances using the same set of parameters, i.e., the angular width of 50°, latitude of 3°and longitude of 1°, as shown on the top of panels. The circle in each panel corresponding to a specific radial distance matches the bright ring observed at an appropriate time. The specific radial distance and the appropriate time is shown on the top of each panel.

[16] A plot of radial distance of the CME versus time is shown in Figure 5, with the data points obtained from the images in Figure 4. For fitting the time-distance scatter points, the Downhill Simplex method is used. The method requires only function evaluations, not derivatives [*Press et al.*, 1994]. The dotted and solid lines in the top panel are obtained using the method based on, respectively, the constant speed and constant acceleration fit to the data points. The bottom panel of Figure 5 displays the inferred speed at various heliocentric distances. The solid curve in the top panel matches the data points better than the dotted line, suggesting it is more likely that the 12 May 1997 CME was accelerating between 08:06 UT and 14:51 UT. It was accelerated from 200 km/s at about 9.5 solar radii to 650 km/s at about 24 solar radii.

5. Summary and Discussion

[17] The halo CME is interpreted here as a broad 3-D shell or bubble of dense plasma ejected near the disk center and propagating radially from the Sun. The 3-D shell or bubble model is actually implicit in the characterization of CMEs as disruptions of an arcade of closed field lines (a cavity) above a magnetic neutral line (usually a prominence) [*Hundhausen*, 1999]. Since many broadside CMEs propagate radially and have constant angular widths, the shape of the observed broad shell can be reproduced by the cone model developed here, if halo CMEs are the same as broadside CMEs except for their central position located far away from the solar limb.

[18] The three free parameters in the cone model characterize the angular width and central position of halo CMEs. They can be determined uniquely using the observed shape of halo CMEs if the halo is not centered exactly on the disk of the Sun. The solution becomes degenerate when the central axis of the cone is aligned with the line of sight, i.e., the central position of the CME is located exactly at the center of the Sun's disk. This degeneracy limits the use of the cone model in determining the geometric and kinematic properties of CMEs ejected from the disk center.

[19] It is found on the basis of the prediction of the cone model that for a CME with angular width of 45 degrees to be a full halo CME, its central position must be within a circle of ~15 degrees from the disk center, and to be a partial halo CME between two circles of ~15 and ~30 degrees. As the angular width of a CME increases, the chance to form a full or partial halo CME also increases.

[20] The cone model has been used to reproduce the 12 May 1997 halo CME observed by the LASCO/C3 coronagraph, suggesting that the halo CME was propagating radially in the C3 field of view and that the angular width of 50.0 degrees remains constant during its propagation through the outer corona. The inferred orientation of the central axis of the cone is at a latitude of 3.0 and longitude of 1.0 degrees, located between the solar disk center and active region 8038 (23N 7W). Since it is located a little bit north of the equator, the halo CME would be expected to be brighter to the north (where it is closer to the sky plane) than to the south. Indeed, the CME appears to be somewhat brighter to the north than to the south (see Figure 3). The halo CME was most likely accelerated from 200 km/s to 650 km/s in 6.75 hours. The front acceleration is about 18.5 m/s^2. The speed in the plane of the sky should be the multiplication of the measured radial speed by sin $(\omega \pm \sqrt{\lambda^2 + \phi^2})$. It ranges from 237 km/s to 307 km/s for the asymptopic radial speed of 650 km/s.

[21] By choosing a specific feature in a time-lapse movie and tracking its position outward with time, two different results are obtained for the 12 May 1997 full halo CME. One is propagating with constant speed of 250 km/s in the plane of the sky [*Plunkett et al.*, 1998]. The other obtains the second order fit speed in the plane of the sky from 335 km/s to 220 km/s with a deceleration of −15.0 m/s^2 (http://cdaw.gsfc.nasa.gov/CME_list/UNIVERSAL/1997_05/univ1997_05.html). The difference of the two results may be caused by choosing different features. The possible bias in tracking a specific feature in different time may also produce some error in this kind of measurement. Using the technique of the synoptic grey-scale map to the 12 May 1997 halo CME, the propagation of the CME in the plane of the sky is found to be accelerated, and asymptopic sky-plane speeds of 314 km/s, 345 km/s, and 402 km/s are obtained for, respectively, the leading edge, center of white, and black and white of the CME [see *Sheeley et al.*, 1999, Table 1].

[22] The synoptic grey-scale map shows the flow pattern along the chosen path as a continuous sequence of height/time tracks whose individual shapes are easily recognized and compared, and free from observational selection and bias. The upward curving track is similar to that obtained using the cone model, confirming the inference of acceleration. The 12 May 1997 halo CME is associated with a

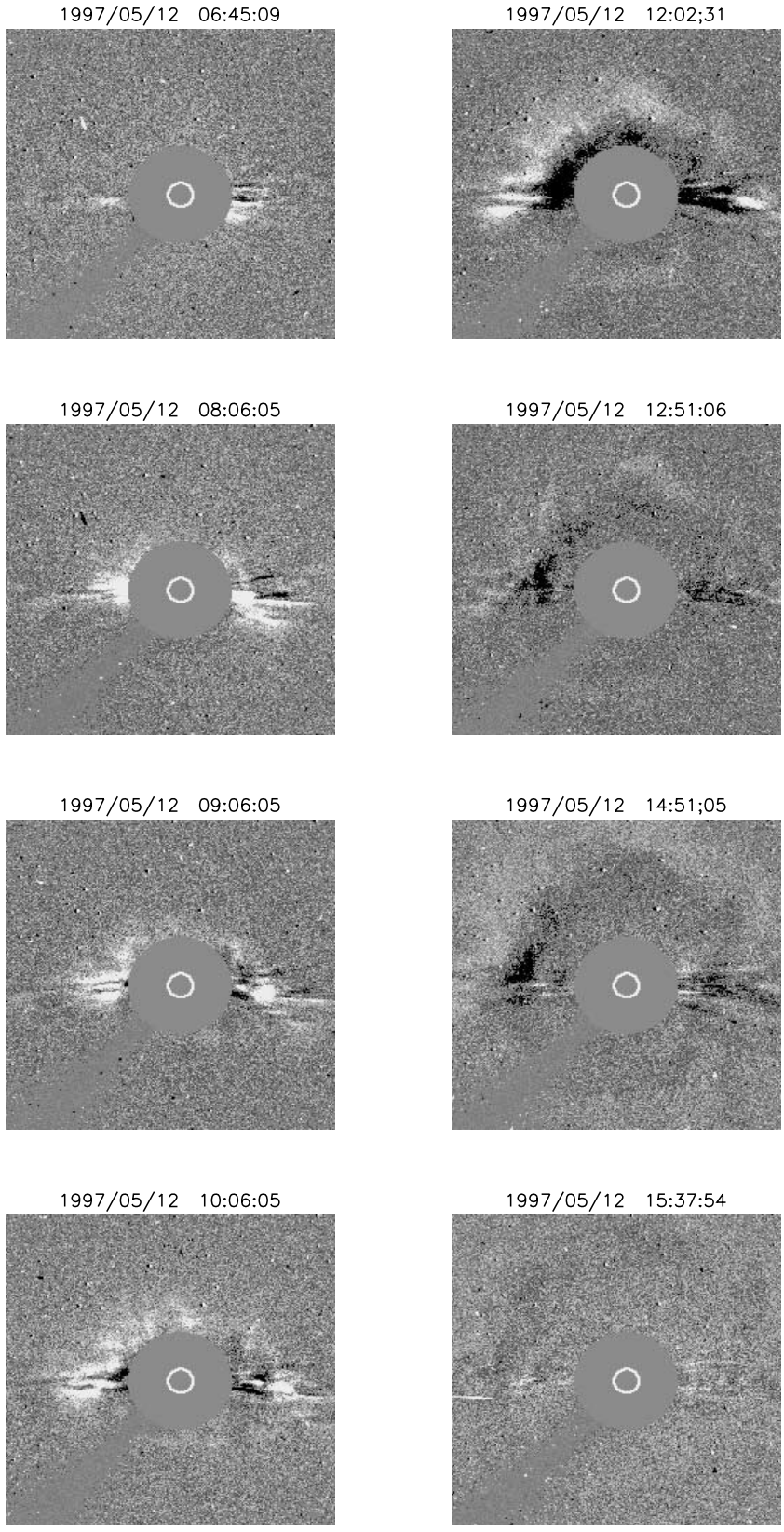

Figure 3. The development of the 12 May 1997 full halo CME observed by LASCOC3. The top of each panel shows the date and time when the image was observed.

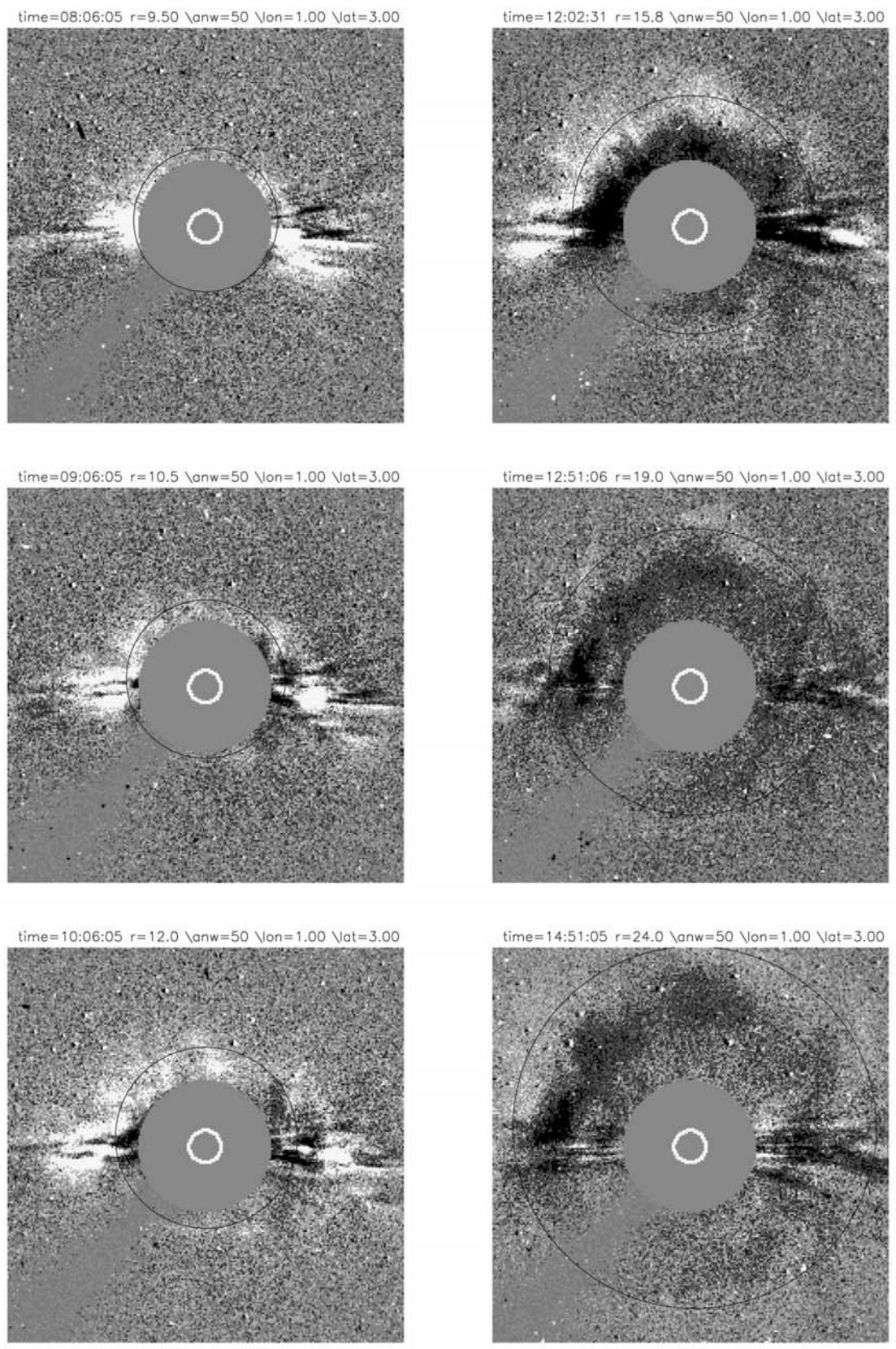

Figure 4. Comparison of predicted halos (dark circles) at different radial distance, r, when anw = 50.0°, lon = 1.0° and lat = 3.0° with observed halos at corresponding times.

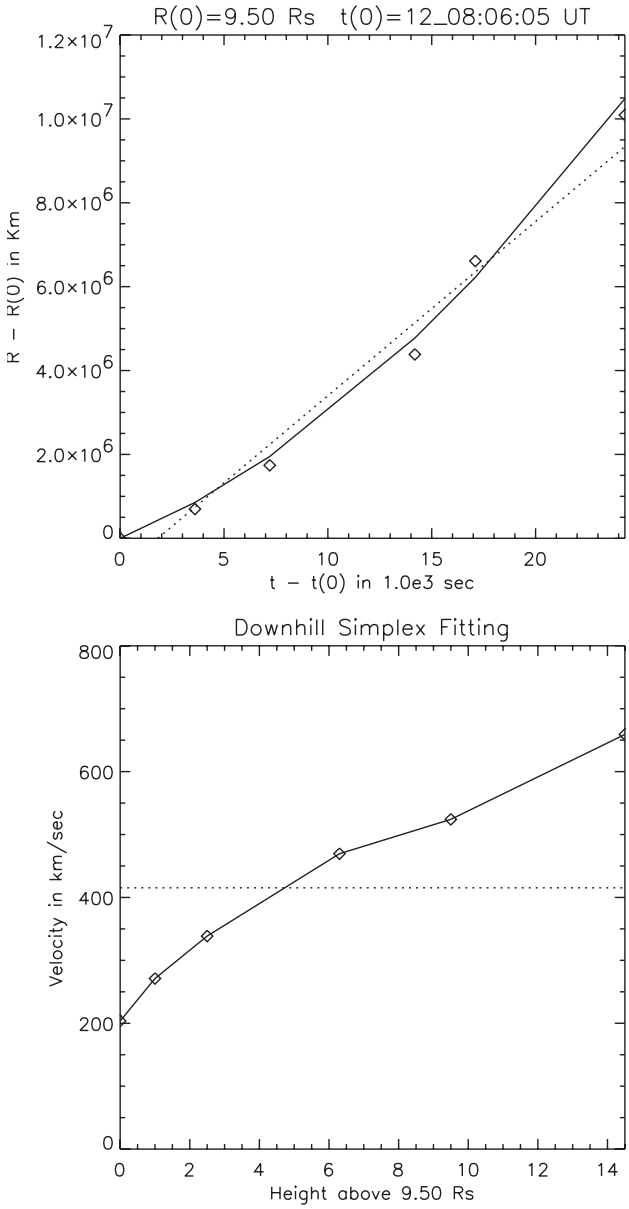

Figure 5. The plot (the top panel) of the inferred series of time and radial distance as shown in the top of each panel of Figure 4. Here R(0) and t(0) are, respectively, the radial distance of 9.5 solar radii and the time of 08:06 UT. The dotted and solid lines are fits obtained using the Downhill Simplex Fitting technique, assuming constant speed and constant acceleration, respectively. The bottom panel shows the radial velocities at various height.

solar filament disappearance (SFD). The SFD associated broadside CMEs have shown to be of "gradual acceleration" [*Sheeley et al.*, 1999]. The asymptopic sky-plane speed of 307 km/s obtained by the cone model slightly differs from that from the technique of the synoptic grey-scale map, it may be caused by using the middle of rather fuzzy rings of the halo CME in the present work. There is uncertainty in identifying the middle of rather fuzzy rings of halo CMEs. This uncertainty may introduce some error in determining the free parameters of the cone model, and thus, the acceleration and speed. A more objective criterion to accurately locate the expanding bright rings of halo CMEs is required, and the synoptic grey-scale map may be helpful in identifying the halo at various time and height.

[23] There are two bright regions near the equator on the east and west limbs in the 12 May 1997 event (see Figure 3). The brightening in the equatorial regions might be caused by deflections and/or compressions of preexisting coronal features back toward the plane-of-the-sky, making them appear brighter in coronagraph images [*St.Cyr and Hundhausen*, 1988]. The two bright regions may also suggest that they are a part of the halo CME, and the cross section of the cone is elliptic, rather than round. An elliptic cone model has been developed recently to reproduce such obviously elliptic halo CMEs.

[24] Not all CMEs have constant angular width and fit the cone model. It is also likely that the origin of CMEs is not near a point on the surface but up into the corona and involves the evacuation of a large volume of coronal material. Some CMEs clearly involve the blowout of a streamer. More examples need to be examined in order to see what fraction of halo CMEs can be reproduced with the cone model.

[25] **Acknowledgments.** Shadia Rifai Habbal thanks Orville Chris St. Cyr and David F. Webb for their assistance in evaluating this paper.

References

Brueckner, G. E., et al., The Large Angle Spectroscopic Coronagraph (LASCO), *Sol. Phys.*, *162*, 357, 1995.

Cane, H. V., I. G. Richardson, and O. C. St. Cyr, The interplanetary events of January–May, 1997, as inferred from energetic particle data, and their relationship with solar events, *Geophys. Res. Lett.*, *25*, 2517, 1998.

Delaboudiniere, J.-P., et al., EIT: Extreme-Ultraviolet Imaging Telescope for the SOHO Mission, *Sol. Phys.*, *162*, 291, 1995.

Fisher, R. R., and R. H. Munro, Coronal transient geometry, 1, The flare-associated event of 1981 March 25, *Astrophys. J.*, *280*, 428, 1984.

Gopalswamy, N., A. Lara, R. P. Lepping, M. L. Kaiser, D. Berdichevsky, and O. C. St. Cyr, Interplanetary acceleration of coronal mass ejections, *Geophys. Res. Lett.*, *27*, 145, 2000.

Harrison, R. A., Solar coronal mass ejections and flares, *Astron. Astrophys.*, *162*, 283, 1986.

Howard, R. A., D. J. Michels, N. R. Sheeley Jr., and M. J. Koomen, The observation of a coronal transient directed at Earth, *Astrophys. J.*, *263*, L101, 1982.

Howard, R. A., N. R. Sheeley Jr., M. J. Koomen, and D. J. Michels, Coronal mass ejections: 1979–1981, *J. Geophys. Res.*, *90*, 8173, 1985.

Hudson, H. S., J. R. Lemen, O. C. St. Cyr, A. C. Sterling, and D. F. Webb, X-ray coronal changes during halo CMEs, *Geophys. Res. Lett.*, *25*, 2481, 1998.

Hundhausen, A. J., Size and locations of coronal mass ejections: SMM observations from 1980 and 1984–1989, *J. Geophys. Res.*, *98*, 13,177, 1993.

Hundhausen, A. J., A summary of SMM observations from 1980 and 1984–1989, in *The Many Faces of the Sun: A Summary of the Results from NASA's Solar Maximum Mission*, edited by K. T. Strong et al., p. 143, Springer-Verlag, New York, 1999.

Jackson, B. V., Helios observations of the Earthward-directed mass ejection of 27 November, 1979, *Sol. Phys.*, *100*, 563, 1985.

Plunkett, S. P., et al., The relationship of green-line transients to white-light coronal mass ejections, *Sol. Phys.*, *175*, 699, 1997.

Plunkett, S. P., et al., LASCO observations of an Earth-directed coronal mass ejection on May 12, 1997, *Geophys. Res. Lett.*, *25*, 2477, 1998.

Plunkett, S. P., et al., Solar source regions of coronal mass ejections and their geomagnetic effects, *J. Atmos. Sol. Terr. Phys.*, *63*, 389, 2001.

Press, W. H., et al., *Numerical Recipes in C: The Art of Scientific Computing*, 2nd ed., p. 408, Cambridge Univ. Press, New York, 1994.

Sheeley, N. R., Jr., J. H. Walters, Y.-M. Wang, and R. A. Howard, Continuous tracking of coronal outflows: Two kinds of coronal mass ejections, *J. Geophys. Res.*, *104*, 24,739, 1999.

St. Cyr, O. C., and A. J. Hundhausen, On the interpretation of "halo" coronal mass ejections, in *Solar Wind Six*, edited by V. Pizzo, T. Holzer,

and D. G. Simes, *Tech. Note NCAR/TN-306+Proc*, p. 356, Natl. Cent. for Atmos. Res., Boulder, Colo., 1988.

St. Cyr, O. C., et al., Properties of coronal mass ejections: SOHO LASCO observations from January 1996 to June 1998, *J. Geophys. Res.*, *105*, 18,169, 2000.

Thompson, B. J., et al., SOHO/EIT observations of an Earth-directed coronal mass ejection on May 12, 1997, *Geophys. Res. Lett.*, *25*, 2465, 1998.

Webb, D. F., and B. V. Jackson, The identification and characteristics of solar mass ejections observed in the heliosphere by the Helios-2 photometers, *J. Geophys. Res.*, *95*, 20,641, 1990.

Webb, D. F., et al., Large-scale structures and multiple neutral lines associated with coronal mass ejections, *J. Geophys. Res.*, *102*, 24,161, 1997.

Webb, D. F., E. W. Cliver, N. U. Crooker, O. C. St. Cyr, and B. J. Thompson, The relationship of halo coronal mass ejections, magnetic clouds, and magnetic storms, *J. Geophys. Res.*, *105*, 7491, 2000.

Webb, D. F., N. U. Crooker, S. P. Plunkett, O. C. St. Cyr, The solar sources of geoeffective structures, in *Space Weather*, *Geophys. Monogr. Ser.*, vol. 125, edited by P. Song, H. J. Singer, and G. L. Siscoe, p. 123, AGU, Washington, D. C., 2001.

Zhao, X. P., and D. F. Webb, Large-scale closed field regions and halo coronal mass ejections, *Eos Trans. AGU*, *81*(48), Fall Meet. Suppl., Abstract SH72B-03, 2000.

W. Liu and X. P. Zhao, W. W. Hansen Experimental Physics Laboratory, Stanford University, Stanford, CA 94305-4085, USA. (weiliu@quake.stanford.edu; xpzhao@solar.stanford.edu)

S. P. Plunkett, USRA, Naval Research Laboratory, Code 7660, Washington, DC 20375, USA. (plunkett@sunrise.nrl.navy.mil)